Electronic Supplementary Material (ESI) for Nanoscale.

Supplementary Information

Engineering Defect State and Reducibility of Ceria Based Nanoparticles for Improved Anti-oxidation Performance

Yan-Jie Wang,[a,b] Hao Dong,[a] Guang-Ming Lyu,[a] Huai-Yuan Zhang,[a] Jun Ke,[a] Li-Qun Kang,[a] Jia-Li Teng,[c] Ling-Dong Sun,[a],* Rui Si,[d] Jing Zhang,[e] Yan-Jun Liu,[c],* Ya-Wen Zhang,[a] Yun-Hui Huang[b],* and Chun-Hua Yan[a],*

[a] *Beijing National Laboratory for Molecular Sciences, State Key Laboratory of Rare Earth Materials Chemistry and Applications, PKU-HKU Joint Laboratory in Rare Earth Materials and Bioinorganic Chemistry, Peking University, Beijing 100871, China. Fax: +86-10-62754179; Tel: +86-10-62754179; E-mail: sun@pku.edu.cn, yan@pku.edu.cn.*

[b] *Key Laboratory for Advanced Battery Materials and System (MOE), School of Materials Science and Engineering, Huazhong University of Science and Technology (HUST), Wuhan, Hubei 430074, China. Fax: +86-27-87558241; Tel: +86-27-87558241; E-mail: huangyh@mail.hust.edu.cn.*

[c] *Department of Endocrinology, 306 Hospital of People's Liberation Army, Beijing 100101, China; Fax: +86-10-64860685; Tel: +86-10-66356374; E-mail: damaoermaosanmao@aliyun.com.*

[d] *Shanghai Synchrotron Radiation Facility, Shanghai Institute of Applied Physics, Chinese Academy of Sciences, Shanghai 201204, China.*

[e] *Beijing Synchrotron Radiation Facility, Institute of high energy physics, Chinese Academy of Sciences, Beijing 100049, China.*

Table S1. Characterization of CeO_2 and CeO_2:Gd NPs.

Sample	[a]Size (nm)	[b]Lattice parameter (pm)	Hydrodynamic Diameter (nm)	[c]Gd^{3+}（XPS）	Gd^{3+}（ICP）	I_{D1}/I_{F2g}
CeO_2	6.64	541	98.1	--	--	0
CeO_2:10%Gd	6.44	545	108.4	9.9%	10.6%	0.023
CeO_2:20%Gd	6.44	546	106.8	20.5%	20.0%	0.075

[a] Particle size calculated by Scherrer equation.

[b] 2θ correction and cell dimension calculation were performed using LAPOD code with least squares refinement (Ref. S2 and S3).

[c] Background excluding, curve fitting, and peak integration were performed using CasaXPS v2.3.15 software. Amount of Gd and Ce were obtained from the peak area (*A*) of Ce 3d, Gd 4d spectra. The doping ratio of Gd atom at surface levels was calculated through the following equation:

$$\mathrm{Gd\%} = \frac{\frac{A(\mathrm{Gd})}{S(\mathrm{Gd})}}{\frac{A(\mathrm{Gd})}{S(\mathrm{Gd})} + \frac{A(\mathrm{Ce})}{S(\mathrm{Ce})}}$$

In which, *S* is the relative sensitivity factor. Uncertainly for the fitting and measurements was estimated to be about ±30%.

Table S2. BET surface area and catalytic performance of CeO_2 and CeO_2:Gd NPs.

Sample	BET surface area / $m^2 \cdot g^{-1}$	Conversion concentration of H_2O_2 at 30min / $mmol \cdot L^{-1}$	Specific reaction rate		TOF at 37 °C / s^{-1}
			per unit weight of catalyst / $mol \cdot h^{-1} \cdot g{-}1$	per unit surface area / $mol \cdot h^{-1} \cdot m^{-2}$	
CeO_2	92	0.47	9.55	0.10	0.60
CeO_2:10%Gd	117	0.61	12.17	0.11	0.66
CeO_2:20%Gd	107	0.71	14.24	0.16	0.95

Table S3. Δλ at optical density of 0.3 of CeO_2 and CeO_2:Gd NPs.

Sample.	CeO_2	CeO_2:10%Gd	CeO_2:10%Gd
Δλ at optical density of 0.3	26	32	36

Table S4. Catalytic performance of CeO_2 and CeO_2:Gd NPs for third cycle.

Sample for third cycle	CeO_2	CeO_2:10%Gd	CeO_2:20%Gd
TOF at 37^oC /s-1	0.40	0.46	0.57

Table S5. The typical EXAFS results of CeO_2:Gd NPs during the anti-oxidation process.

Sample.	Shell	CN	*R* / Å	σ^2 / $Å^2$
CeO_2:10Gd	Ce-O	5.7 ±0.3	2.315 ±0.005	0.009 ±0.001
CeO_2:20Gd	Ce-O	5.5 ±0.3	2.303 ±0.005	0.010 ±0.001
CeO_2:20Gd-10min	Ce-O	6.4 ±0.2	2.312 ±0.001	0.012 ±0.001
CeO_2:20Gd-3h	Ce-O	6.0 ±0.3	2.303 ±0.006	0.011 ±0.001
CeO_2:20Gd-9h	Ce-O	6.0 ±0.2	2.302 ±0.005	0.011 ±0.001

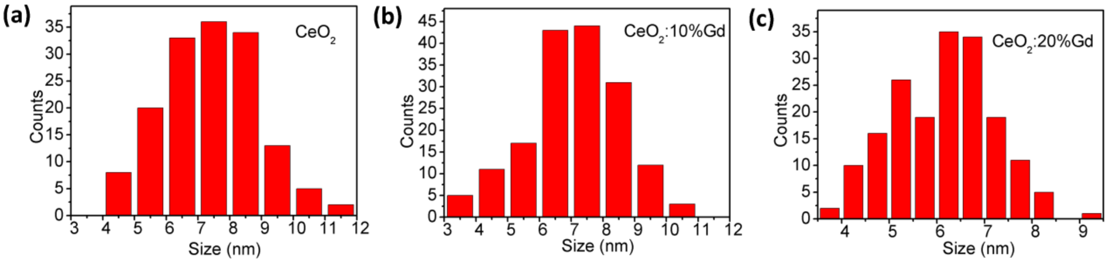

Fig. S1. Size distribution of CeO_2-based NPs from TEM image. (a) CeO_2 NPs. (b) CeO_2:10%Gd NPs. (c) CeO_2:20%Gd NPs.

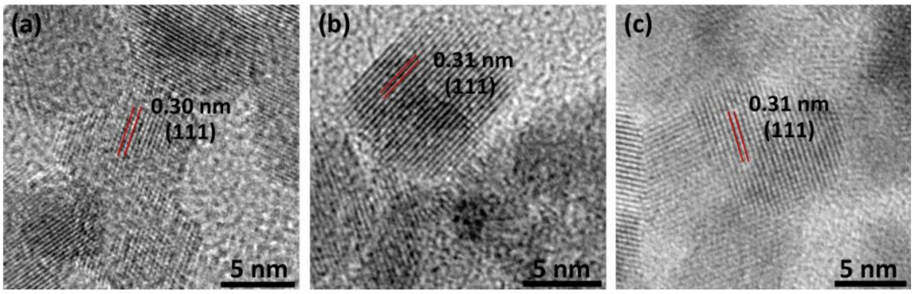

Fig. S2. HRTEM images of CeO_2-based NPs. (a) CeO_2 NPs. (b) CeO_2:10%Gd NPs. (c) CeO_2:20%Gd NPs.

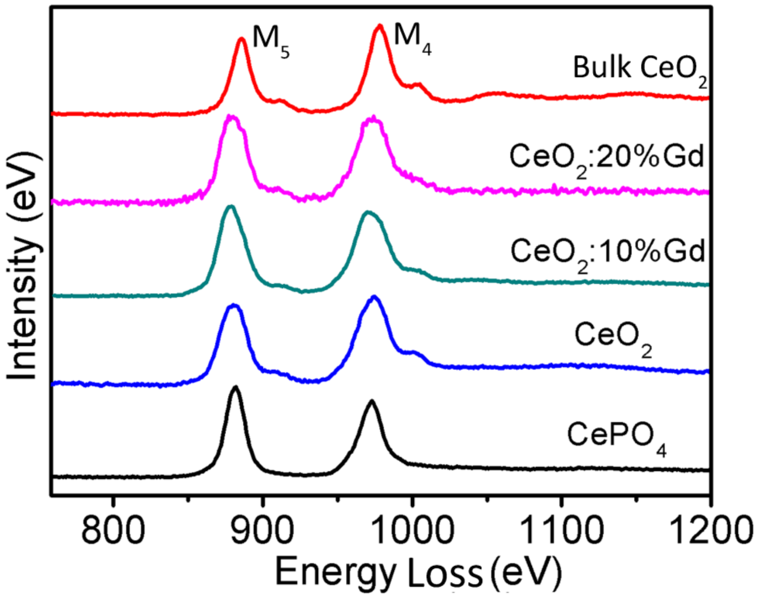

Fig. S3. [a]EELS spectra of CeO_2-based NPs. For comparison, $CePO_4$ and bulk CeO_2 were also detected by EELS. The $M_{4,5}$ edges reflect transitions of 3d core electrons to unoccupied states of p-and f-like symmetry. The spectra of CeO_2 and CeO_2:Gd are close to that of bulk CeO_2. The Ce^{3+}/Ce^{4+} ratios can be determined by comparing M_4/M_5 intensity ratio. The spectrum of bulk CeO_2 gives a M_4/M_5 intensity ratio of 0.93, which is the characteristic of Ce^{4+}, the spectrum of $CePO_4$ gives a M_4/M_5 intensity ratio of 1.38, which is the characteristic of Ce^{3+}. Meanwhile, as-prepared CeO_2, gives a ratio of 1.0, indicating that a small number of Ce^{3+} (about 15%) exists. Similarly, the fraction of Ce^{3+} in CeO_2:10%Gd and CeO_2:20%Gd NPs is respectively 40%, 35%.

[a] The EELS acquisition time is about 10 s

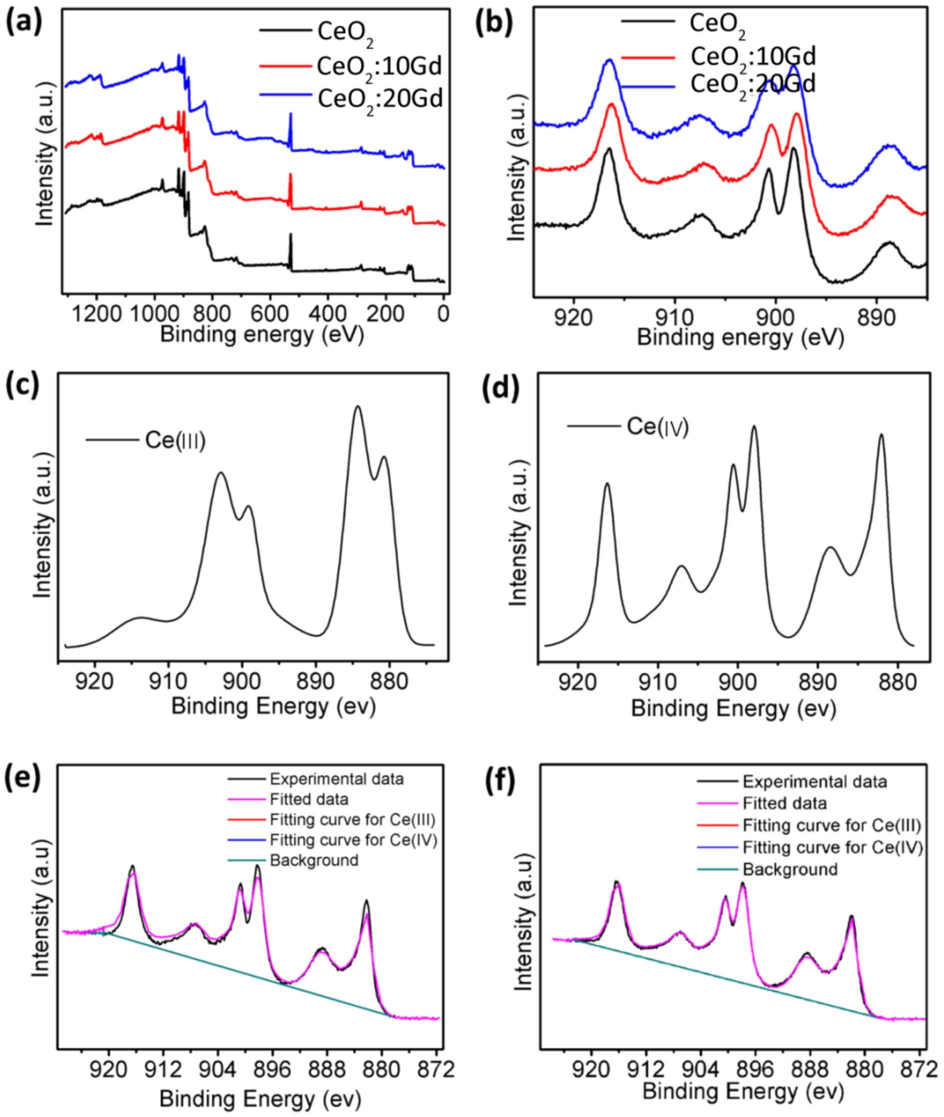

Fig. S4. XPS spectra of as-prepared CeO_2-based NPs. (a) Full XPS spectra of CeO_2 and CeO_2:Gd NPs. (b) Ce 3d spectra of CeO_2 and CeO_2:Gd NPs. (c) Ce 3d XPS spectrum of Ce(III). (d) Ce 3d XPS spectrum of Ce(IV). Standard Ce(III) and Ce(IV) were obtained from CeO_2 and Ce_2O_3. They were used to fit Ce 3d spectra to obtain Ce(III) proportion. (e) Ce 3d spectra of CeO_2 NPs fitted as the linear combination of Ce(III) and Ce(IV) 3d spectra with the reported method (Ref. S1). (f) Ce 3d spectra of CeO_2:20%Gd nanoparticles fitted as the linear combination of Ce(III) and Ce(IV) 3d spectra with the reported method (Ref. S1).

There is no obvious difference in the Ce 3d XPS spectrum after doping Gd^{3+} into CeO_2 NPs. From the fitting results, Ce 3d XPS spectra of three CeO_2 based NPs are close to Ce^{4+}, indicating that the main valance of surface Ce in the sample is +4, probably due to the synthesis of CeO_2 NPs in oxygen-enriched environment.

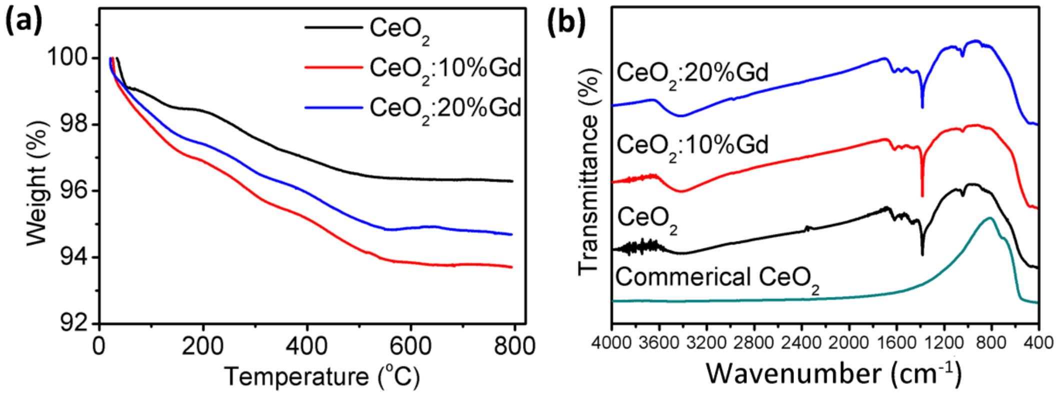

Fig. S5. (a) TG curves of CeO_2 and CeO_2:Gd NPs. (b) FT-IR spectra of CeO_2 and CeO_2:Gd NPs. The weight loss of CeO_2, CeO_2:10%Gd and CeO_2:20%Gd and is 3.7%, 6.3% and 5.3%, respectively. The weight loss is proposed to be due to the surface bound-OH and residual NO_3^-. The peak nearby 3430 cm^{-1} shown in FT-IR spectra of CeO_2 based NPs is proposed to be attributed to the stretching vibration of the surface bound-OH. In addition, the surface bound-OH could increase after doping Gd^{3+} into the CeO_2 based NPs from the FT-IR spectra.

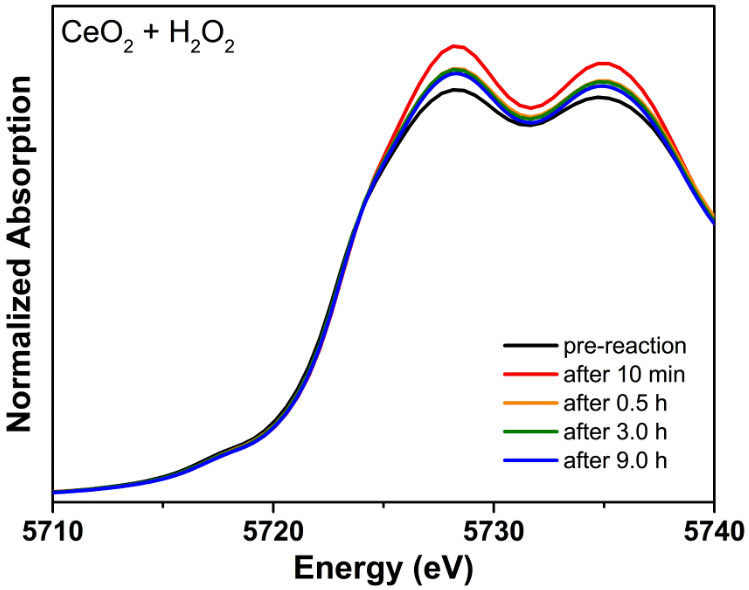

Fig. S6. The Time-dependent XANES spectra of CeO_2 NPs during the reaction with H_2O_2. Every XAFS spectrum was collected for 10 times to improve the data accuracy. There is no obvious difference in the XANES spectra of CeO_2 NPs following the reaction.

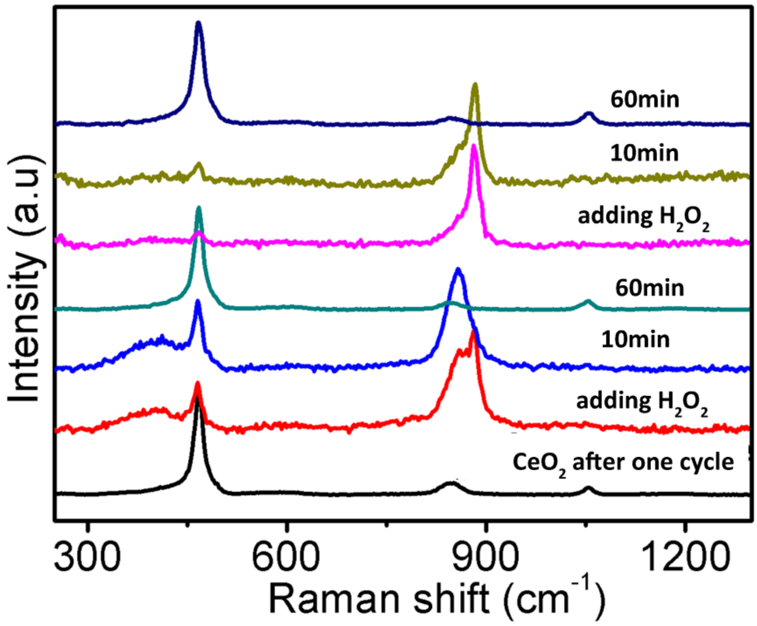

Fig. S7. Raman spectra of prepared CeO_2 NPs during the reaction with H_2O_2 for the second and third cycle.

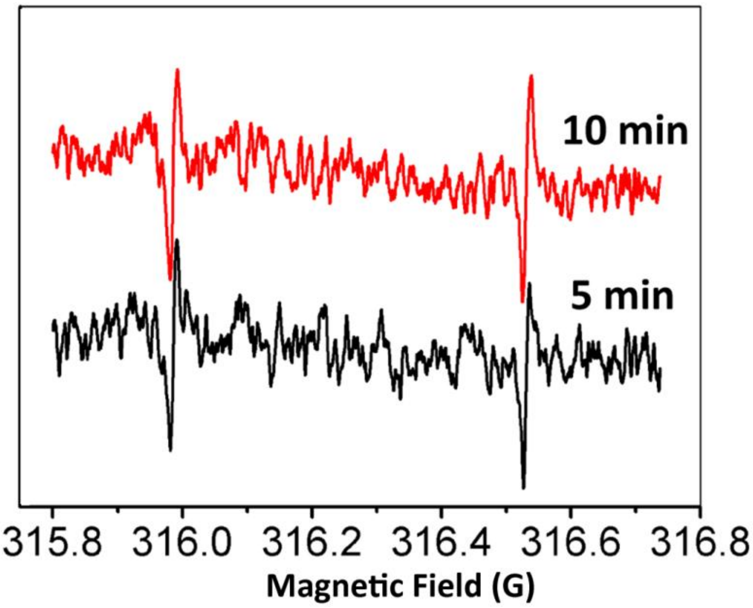

Fig. S8. EPR spectra of the reaction system including 100 μg/mL CeO_2 and 80 μg/mL H_2O_2. The black: at the beginning of the reaction, the red: reaction for 10min.

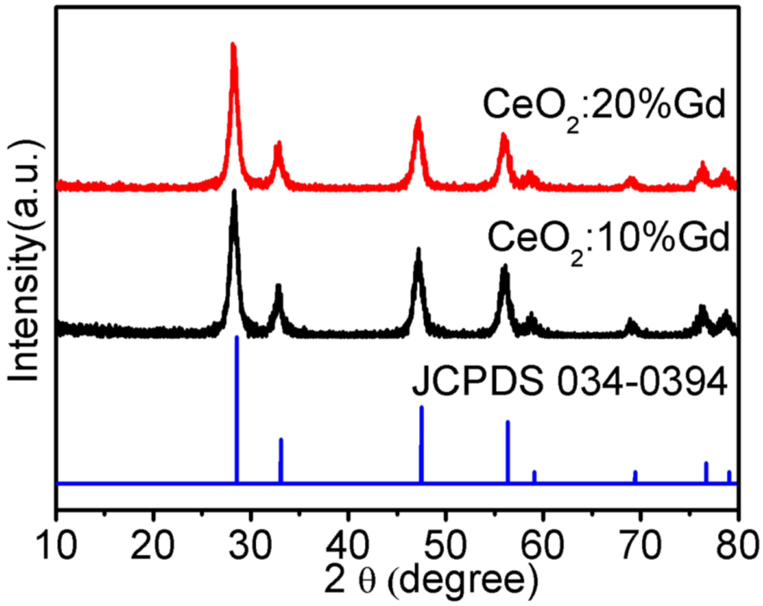

Fig. S9. XRD spectra of CeO_2:Gd NPs.

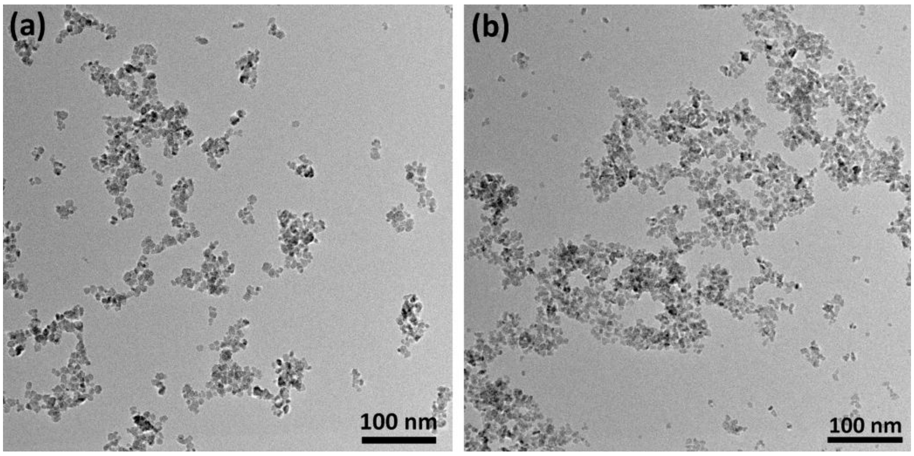

Fig. S10. TEM images of CeO_2:Gd NPs. (a) CeO_2:10%Gd NPs. (b) CeO_2:20%Gd NPs.

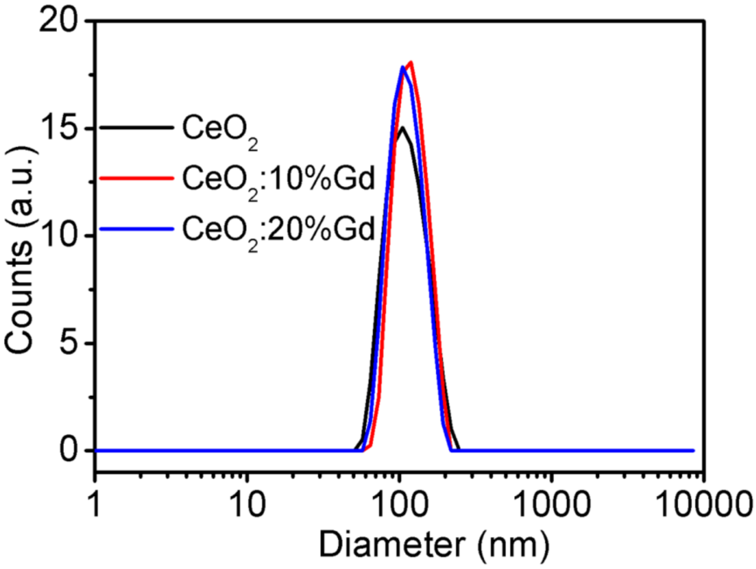

Fig. S11. Hydrodynamic diameter of CeO_2-based NPs.

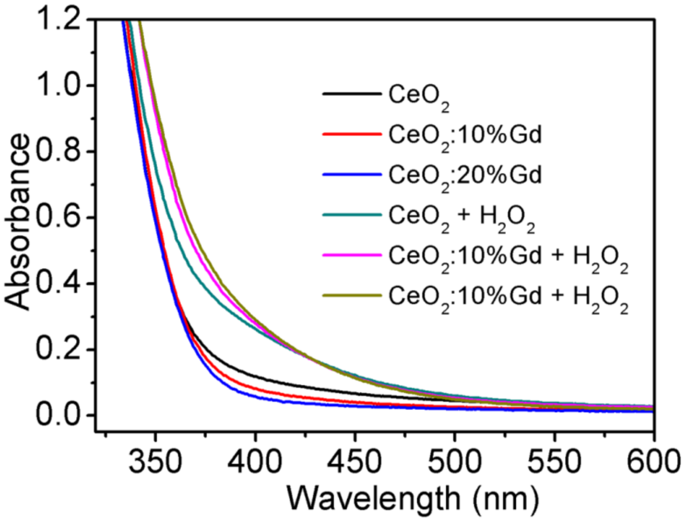

Fig. S12. UV-vis absorption spectra of CeO_2 and CeO_2:Gd NPs before and after the addition of excess H_2O_2 (H_2O_2/Ce ratio was 57).

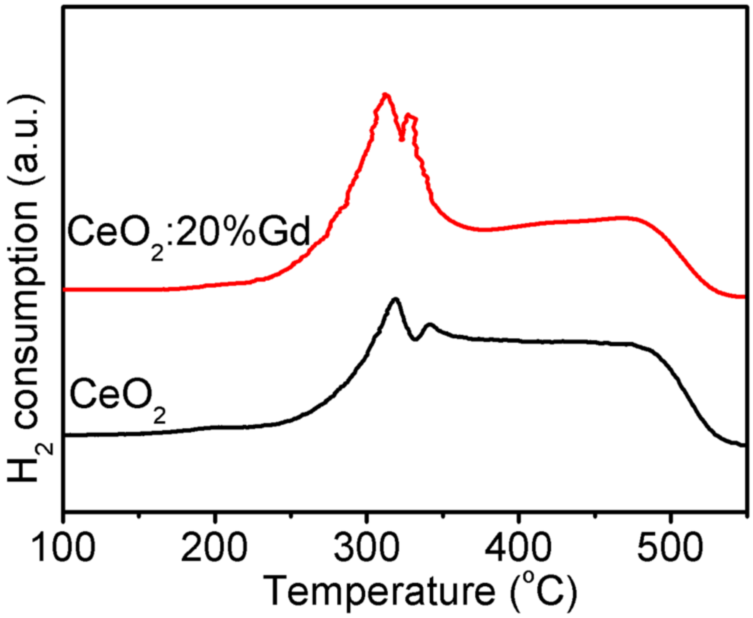

Fig. S13. H_2-TPR analysis over CeO_2 and CeO_2:Gd NPs.

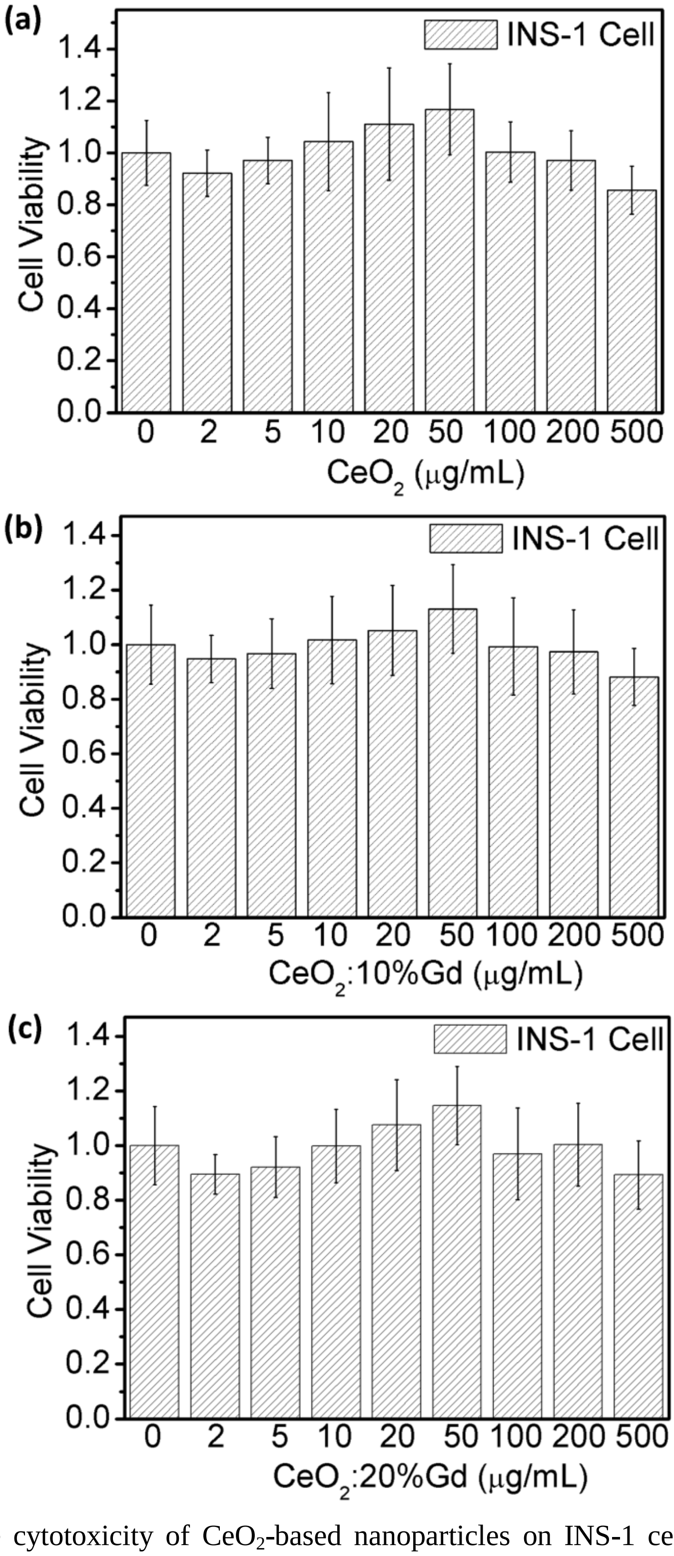

Fig. S14. *In vitro* cytotoxicity of CeO_2-based nanoparticles on INS-1 cells for 3 days. (a) CeO_2 NPs. (b) CeO_2:10%Gd NPs. (c) CeO_2:20%Gd NPs.

References

[S1] C. Zhang, M. E. Grass, A. H. McDaniel, S. C. DeCaluwe, F. E. Gabaly, Z. Liu, K. F. McCarty, R. L. Farrow, M. A. Linne, Z. Hussain, G. S. Jackson, H. Bluhm, and B. W. Eichhorn, *Nature Mater.*, 2010, **9**, 944-949.

[S2] J. I. Langford, J. I. J. *Appl. Crystallogr.*, 1971, **4**, 259-260.

[S3] J. I. Langford, Appl. *Crystallogr.*, 1973, **6**, 190-196.